

Initiating Lane and Band Formation in Heterogeneous Pedestrian Dynamics

Basma Khelfa¹ · Raphael Korbmacher¹ · Andreas Schadschneider² · Antoine Tordeux¹

¹ School for Mechanical Engineering and Safety Engineering, University of Wuppertal, Wuppertal, Germany,

E-mail: khelfa@uni-wuppertal.de, korbmacher@uni-wuppertal.de, tordeux@uni-wuppertal.de

² Institute for Theoretical Physics, University of Cologne, Cologne, Germany,

E-mail: as@thp.uni-koeln.de

Received: 19 August 2021 / Last revision received: 4 October 2021 / Accepted: 15 December 2021

DOI: [10.17815/CD.2021.129](https://doi.org/10.17815/CD.2021.129)

Abstract Self-avoiding agents such as pedestrians or road vehicles can exhibit different types of collective and coordinated dynamics. Prominent examples are stop-and-go waves and lane formation, or nonuniform patterns and ordered structures at bottlenecks and intersections. Non-linear effects, phase transitions, and metastability in the collective dynamics of interacting agents raise interesting theoretical questions. Besides scientific interests, understanding and controlling collective performances from individual interaction rules is fundamental to authorities. In this contribution, we show using a two-species agent-based model that heterogeneity can generically initiate segregation and spontaneous formation of lanes and bands. Two universal heterogeneity mechanisms are identified. In the first one, we attribute statically two different values to the parameters of the two types of agents. We aim here to model static heterogeneous individual characteristics. In the second model, we attribute dynamically two different values for the parameters according to the type of the closest agent in front. In contrast to the first model for which the heterogeneity lies statically in agent characteristics, we aim to model dynamic heterogeneity in the interactions. Simulation results show that self-organized lane and band formations spontaneously occur when the heterogeneity factors are sufficiently high. More precisely, we observe the emergence of longitudinal lanes when the heterogeneity lies in the agents when transversal bands arise if we assume heterogeneity in the interactions. The different organizations of the flow highly influence the system's performance. Lane patterns significantly improve the flow, while band formation acting as gridlocks result in lower performance.

Keywords Pedestrian and evacuation dynamics · static and dynamic heterogeneity · phase transition · collective dynamics · lane formation · band formation · simulation

1 Introduction

The interactions of pedestrians or vehicles in crowds and traffic flows lead to a large variety of complex self-organization phenomena. An important part of this research consists of identifying generic underlying mechanisms and parameters for the emergence of collective dynamics and of developing models describing systemic phase transitions. A typical example of collective dynamics is jamming and clogging phenomena occurring for high densities [1–4]. The jamming effect mainly results from exclusion principle. This phenomenon does not depend strongly on the microscopic dynamics of the particles. Similarly, clogging phenomena are close to the phenomenon of arching occurring in granular materials through narrow openings.

Other classical examples of collective dynamics and self-organisation are lane formation for counter flows [5, 6], herding effect [7, 8], stop-and-go waves [9, 10], freezing-by-heating effect [7, 11] or oscillations, intermittent flow, and pattern formation at bottlenecks and intersections [12–14]; see the reviews [15–17]. Similar collective dynamics arise in social systems, social networks and opinion formation [18–20]. The macroscopic collective effects reflect indirectly the microscopic interactions between the autonomous individuals. Understanding the complex non-linear dynamics taking place between the different modelling levels is challenging and currently attracts much attention [21, 22].

Besides scientific interests, identifying microscopic mechanisms and features allowing initiating macroscopic self-organization is fundamental for the development of intelligent management strategies [23]. Indeed, the collective phenomena initiated by behavioral and social rules of pedestrians or road drivers can lead to improvement or deterioration of the system performance. An typical example of improvement is lane formation for counter flows [5, 24–26] or for unidirectional flows with different desired speeds [27, 28]. The organization in lanes allows to avoid frontal conflicts and, by the way, to improve the streaming. In such a case, we may refer to *intelligent collective dynamics*. Such a concept is also of practical relevance, e.g. for the development of safe and robust autonomous driving systems [29]. Yet, self-organization may also induce deterioration of safety and performance, for instance through stop-and-go waves, herding, clogging effects, and other segregation phenomena [2, 3, 8, 9, 30].

In pedestrian dynamics, collective motion generally results from heterogeneity effects, upon other inertia and reaction-diffusion mechanisms. For instance, lane formation results from universal mechanisms based on heterogeneity of the agent velocities [5, 27, 28]. Other similar examples are stripes, chevrons and travelling band formation for intersecting flows [12–14]. In this contribution, we show by simulation that heterogeneity effects can generically initiate segregation and spontaneous formation of lane or band patterns in two-species flows of polarised agents. Two universal heterogeneity mechanisms are identified: static heterogeneity in the agent characteristics and dynamic heterogeneity in the interactions. Interestingly, lanes spontaneously occur when the heterogeneity relies statically in the agent features, while bands emerge if the heterogeneity operates dynamically in the interactions.

The contribution is organized as follows. We define a two-species pedestrian model, the two types of heterogeneity, and the order parameters we use to quantify the pres-

ence of bands or lanes in Sec. 2. We then present simulation results showing non-linear phase transitions from disorder to order states with lane or band patterns in Sec. 3 before concluding in Sec. 4.

2 Models and analysis

We consider in the following two types of agents evolving on a torus and denote $n = 1, \dots, N$ the agent's ID, \mathbf{x}_n the agent's position, while $k_n = 1, 2$ is the agent's type. The agent's motion is given by a collision-free speed model $F_{\mathbf{p}}(\mathbf{X}_n)$ [31] that defines the agent speed according to local spatio-temporal variables \mathbf{X}_n (the spacing with the neighbours) and a set of parameters \mathbf{p} (e.g., desired speed, desired time gap, agent size, and so on). The agent dynamic is polarised, i.e. all the agents have identical desired direction.

2.1 Pedestrian motion model

In the collision-free speed model for pedestrians [31], the dynamics of an agent n with position \mathbf{x}_n is given by the first order differential equation

$$\dot{\mathbf{x}}_n = M_{\mathbf{p}}(\mathbf{X}_n) = \frac{1}{C} \mathcal{V}(s_n(\mathbf{X}_n)) \left(\mathbf{e}_0 + A \sum_{m \neq n} \exp((\ell - \|\mathbf{x}_n - \mathbf{x}_m\|)/B) \mathbf{e}_{nm} \right). \quad (1)$$

Here, $\mathcal{V} : \mathbb{R}_+ \mapsto \mathbb{R}_+$ is the optimal velocity function defined below, $s_n(\mathbf{X}_n) = \|\mathbf{x}_n - \mathbf{x}_{m_0(\mathbf{X}_n)}\|$ is the minimal distance in front, while \mathbf{e}_0 is the desired direction (polarity), $A, B > 0$ are parameters for the repulsion with the neighbours, \mathbf{e}_{nm} being the direction from agent m to agent n , and $C > 0$ is a normalisation constant. Denoting \mathbf{e}_n the agent direction, the closest agent in front is the agent

$$m_0(\mathbf{X}_n) = \arg \min_{m \in N_n} \|\mathbf{x}_n - \mathbf{x}_m\| \quad (2)$$

with $N_n = \{m, \mathbf{e}_n \cdot \mathbf{e}_{nm} \leq 0 \text{ and } |\mathbf{e}_n^\perp \cdot \mathbf{e}_{nm}| \leq \ell / \|\mathbf{x}_n - \mathbf{x}_m\|\}$, see Fig. 1, and $\arg \min_{m \in N} x_m$ the operator reporting the index m minimising x_m over $m \in N$. The optimal velocity function is the piece-wise linear relationship between speed and spacing

$$\mathcal{V} : s \mapsto \max \{0, \min \{V, (s - \ell)/T\}\}. \quad (3)$$

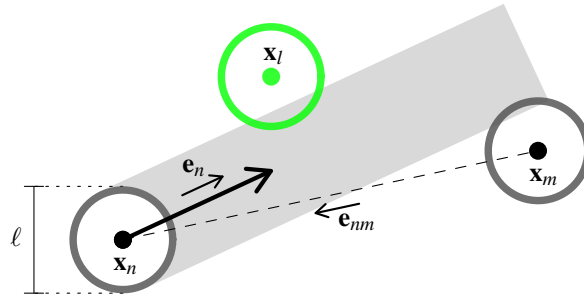


Figure 1 Illustration for the closest agent in front. Here the agent l is the closet agent in front of the agent n .

The parameters are the desired speed $V \geq 0$, the agent size $\ell \geq 0$ and the desired time gap $T > 0$. The default values for the parameters \mathbf{p} are [31]

$$\ell = 0.3 \text{ m}, \quad V = 1.5 \text{ m/s}, \quad T = 1 \text{ s}, \quad A = 5, \quad B = 0.1 \text{ m}. \quad (4)$$

2.2 Heterogeneity types

We assume two different settings \mathbf{p}_1 and \mathbf{p}_2 for the parameters and consider two mechanisms of heterogeneity.

1. In the first heterogeneity model, we attribute statically the two parameter settings \mathbf{p}_1 and \mathbf{p}_2 to the two types of agents:

$$H_1(n, k_n) = M_{\mathbf{p}_{k_n}}(\mathbf{X}_n). \quad (5)$$

We aim here to model different types of agents, for instance pedestrians and bicycles, with specific characteristics in term of desired speed, agent size, etc. It refers to static heterogeneity features remaining constant over the time [32, 33].

2. In the second heterogeneity model, we attribute dynamically the two parameter settings \mathbf{p}_1 and \mathbf{p}_2 according to the type of the closest agent in front. The parameter setting being \mathbf{p}_1 if the agent in front is of the same type and \mathbf{p}_2 otherwise:

$$H_2(n, k_n) = \begin{cases} M_{\mathbf{p}_1}(\mathbf{X}_n), & \text{if } \tilde{k}(\mathbf{X}_n) = k_n, \\ M_{\mathbf{p}_2}(\mathbf{X}_n), & \text{otherwise,} \end{cases} \quad (6)$$

with $\tilde{k}(\mathbf{X}_n)$ the type of the closest agent in front (see Eq. (2)). Such a case may correspond to a pedestrian adapting his/her behaviour when interacting with a bicycle. The heterogeneity features are time-dependent.

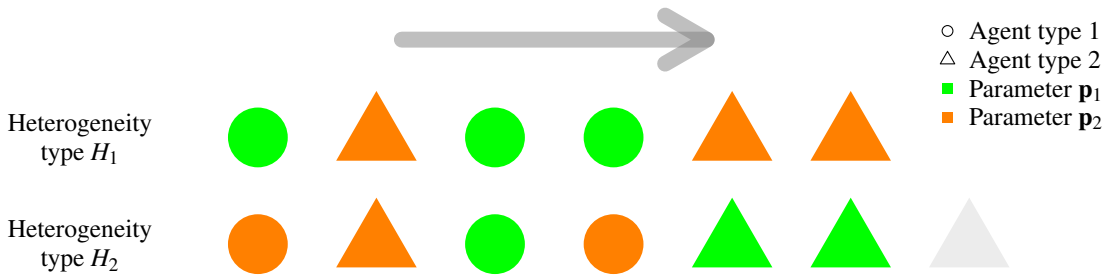


Figure 2 Illustration of the different types of heterogeneity in a one-dimensional case (the arrow indicates the direction of motion). Different shapes (disc and triangle) correspond to different types of agents. The colors (orange and green) represent the parameter setting. Model (5) is heterogeneous in the parameter setting and in model (6) the heterogeneity is in the interactions which depend on the type of agent directly in front: the setting is green when the agent in front is of the same type and orange if it is of a different type.

One important difference between the two models (5) and (6) is the implementation of heterogeneity. Model (5) is heterogeneous in the agent characteristics whereas in model (6) the heterogeneity is in the interactions (see Fig. 2 for an illustrative example in one dimension).

2.3 Order parameter

The static heterogeneity model (5) tends to initiate the formation of lanes in the system, while the dynamic heterogeneity model (6) allows the formation of bands (see Fig. 3 below). The lane and band formation can be described in a quantitative way by suitable order parameters. For detecting lane formation we use the order parameter [34]

$$\Phi_L = \frac{1}{N} \sum_n \phi_n^L \quad \text{with} \quad \phi_n^L = \left[\frac{L_n - \bar{L}_n}{L_n + \bar{L}_n} \right]^2, \quad \left\{ \begin{array}{l} L_n = \#(m, |y_n - y_m| < \Delta, k_n = k_m) \\ \bar{L}_n = \#(m, |y_n - y_m| < \Delta, k_n \neq k_m) \end{array} \right. . \quad (7)$$

Here, ϕ_n^L is the order parameter associated with agent n and $\Delta > 0$ is the width of the lane. L_n denotes the number of agents on the lane in front of the agent n with the same type as the agent n while \bar{L}_n is the number of agents of different type, $\#(A)$ being the operator measuring the number of elements of the set A . The order parameter Φ_L tends to be close to one when the system describes lanes and is close to zero when the flow describes bands (see Fig. 3).

For band formation, the order parameter is

$$\Phi_B = \frac{1}{N} \sum_n \phi_n^B \quad \text{with} \quad \phi_n^B = \left[\frac{B_n - \bar{B}_n}{B_n + \bar{B}_n} \right]^2, \quad \left\{ \begin{array}{l} B_n = \#(m, |x_n - x_m| < w/h \Delta, k_n = k_m) \\ \bar{B}_n = \#(m, |x_n - x_m| < w/h \Delta, k_n \neq k_m) \end{array} \right. . \quad (8)$$

It includes a scaling term w/h allowing to obtain identical distributions for the lane and band order parameters in case of uniform distribution of the agents.

3 Simulation results

We carry out simulations of two-species flows on a 9×5 m rectangular with top-down and right-left periodic boundary conditions using explicit Euler numerical scheme with a time step $\delta t = 0.01$ s. We simulate from random initial conditions the evolution of $N = 45$ agents (density of 1 agent/m²). The simulations are repeated 1000 times from independent random initial conditions for the two heterogeneity types H_1 Eq. (5) and H_2 Eq. (6) with different parameter settings \mathbf{p}_1 and \mathbf{p}_2 . Starting from the default values (T, V) of the parameters Eq. (4), we vary the time gap T and desired speed V in 20 steps to reproduce a heterogeneity of agent speed characteristics. The parameter T ranges into $[0.05, 1.95]$ s by step of 0.05 s, while V ranges into $[1.025, 1.975]$ m/s by step of 0.025 m/s. Denoting (T_1, V_1) the parameters of the setting \mathbf{p}_1 and (T_2, V_2) the parameters of the setting \mathbf{p}_2 , we repeat simulations with

$$T_1 = T + 0.05\delta, \quad T_2 = T - 0.05\delta \quad (9)$$

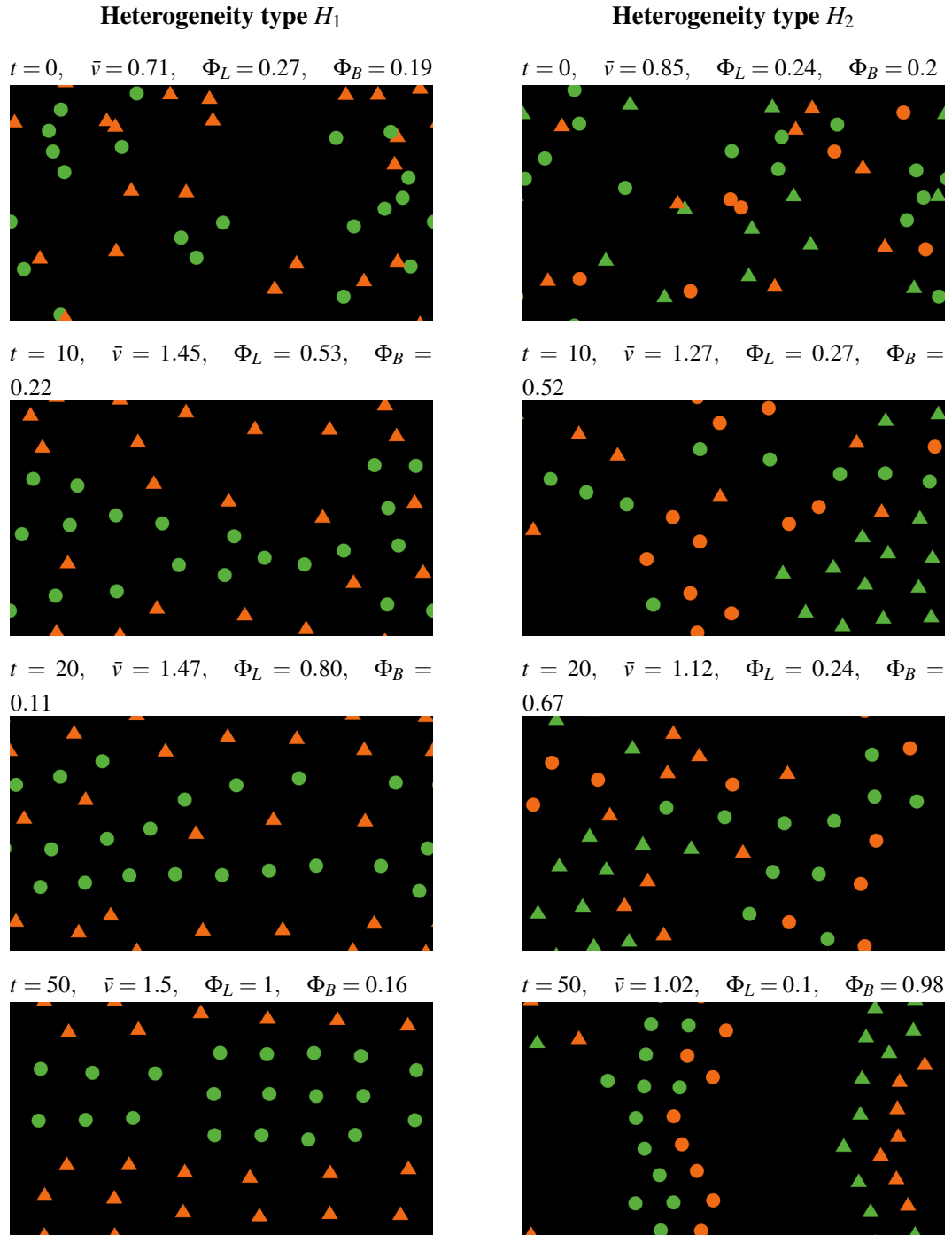


Figure 3 Typical screenshots for the model (5) with heterogeneity in the agent characteristics for which lanes emerge: the lane order parameter Φ_L tends to one while the band order parameter Φ_B tends to zero (left panels, $\delta = 18$), and for the model (6) with heterogeneity in the interactions where bands emerge (right panels, $\delta = 10$). Flow direction from left to right, periodic boundary, and random initial conditions.

and

$$V_1 = V - 0.025\delta, \quad V_2 = V + 0.025\delta \quad (10)$$

for heterogeneity index $\delta = 0, \dots, 19$. Such a ranging relies on the x-axis in the following figures. We measure during the average speeds and average order parameters after a simulation time $t_0 = 600$ s. In Figs. 4–7, we present the mean value with standard deviation bands of system mean speed and order parameter.

3.1 Stationary states

In the simulations, we find that lanes emerge for the case of heterogeneity in the agent characteristics (model (5), see Fig. 4, left panels). On the other hand, band formation is observed for dynamical heterogeneity in the interactions (model (6), see Fig. 4, right panels). If the heterogeneity is increased, an abrupt phase transition occurs from a disordered

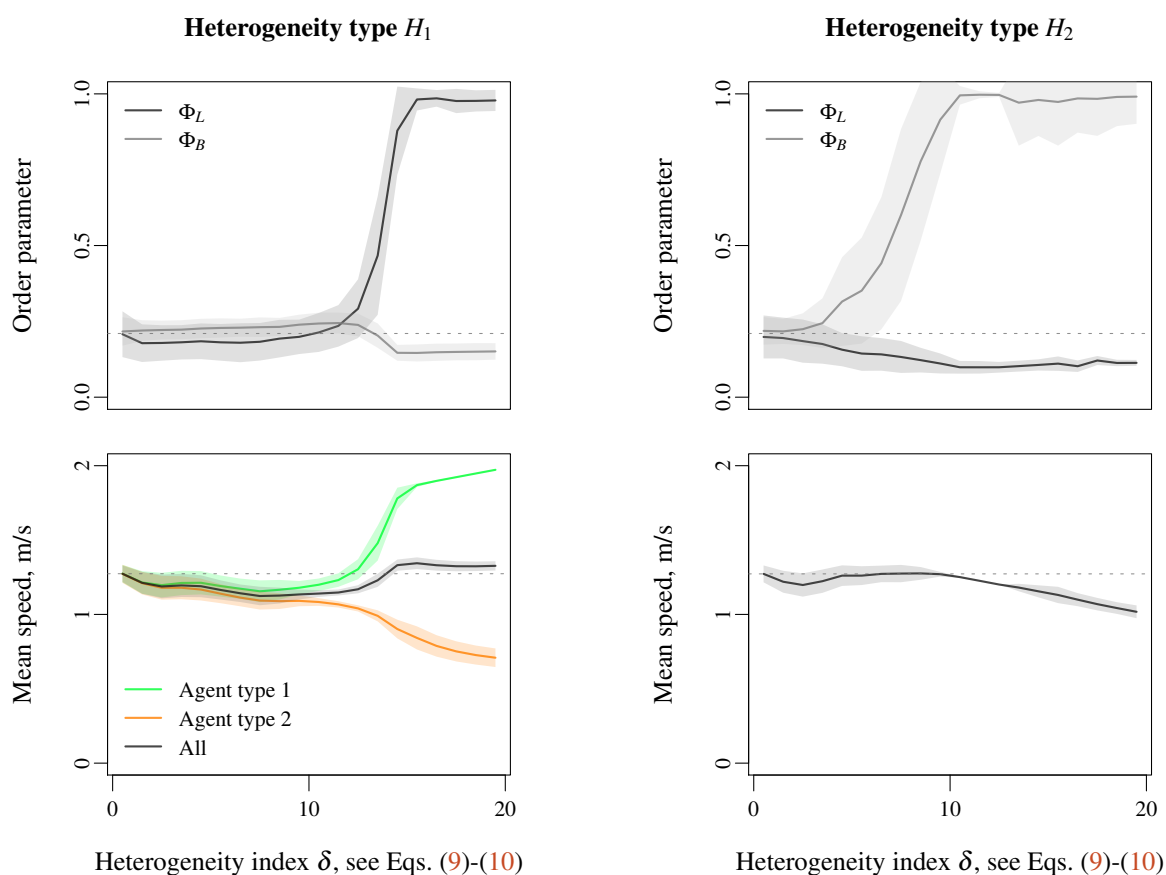


Figure 4 Order parameter for lane and band formation (top panels) and mean speed (bottom panels) according to heterogeneity of agent time gap and desired speed. Horizontal lanes emerge (Φ_L tends to 1 while Φ_B tends to 0) with the model (5) for which the heterogeneity relies on agent characteristics (left panels), while vertical bands appear (Φ_B tends to 1 while Φ_L tends to 0) with the model (6) for which the heterogeneity operates in the interaction (right panels).

distribution of the agents to an ordered dynamics with lanes or bands. The order parameters change from values close to 0.2 (dotted line in Fig. 4, top panels) to a fully polarized state with order parameters close to 0 or 1. Lanes allow that agents with faster characteristics can move with higher speed than those with slower characteristics (Fig. 4, bottom left panel). Thus the agent speed is on average close to the mean speed of a homogeneous flow (dotted line). The band configuration, on the other hand, acts as pseudo-gridlock for which the speed of all the agents have slower features (Figs. 4, bottom right panel).

3.2 Transient states

We now investigate the transient state of the system. We aim first to determine the time required for the emergence of lanes and bands in the systems and when can we consider the system in the stationary state. Fig. 5 shows the curves of the order parameters measured at different simulation times $t_0 = 0, 60, 600, 1200$ and 3000 s according to the heterogeneity index. The lane and band formation occurs spontaneously already in the first minutes of simulation. Furthermore, the curves approximately overlap from $T_0 \geq 600$ s meaning that the system can be considered stationary at this time.

To achieve a deeper understanding of the self-organization features we analyse the robustness of the collective motion against random perturbations. Fig. 6 shows the order parameter when agent speeds are subject to independent Brownian noises with amplitudes $\sigma = 0.1, 0.2$ and 0.5 m/s. The noise systematically perturbs the lane formation for the static heterogeneity model (5) (Fig. 6, left panel). This phenomenon is known in the literature as freezing-by-heating effect [7] in the context of pedestrian dynamics using a concept borrowed from plant growth stimulation process [35]. Related counter-intuitive effects can be observed in other equilibrium and nonequilibrium systems as well [11, 36–40]. On the contrary, noising the dynamics allows improving the band formation in the dynamic heterogeneity model (6) (Fig. 6, right panel, $\sigma = 0.1$ and 0.2 m/s), before

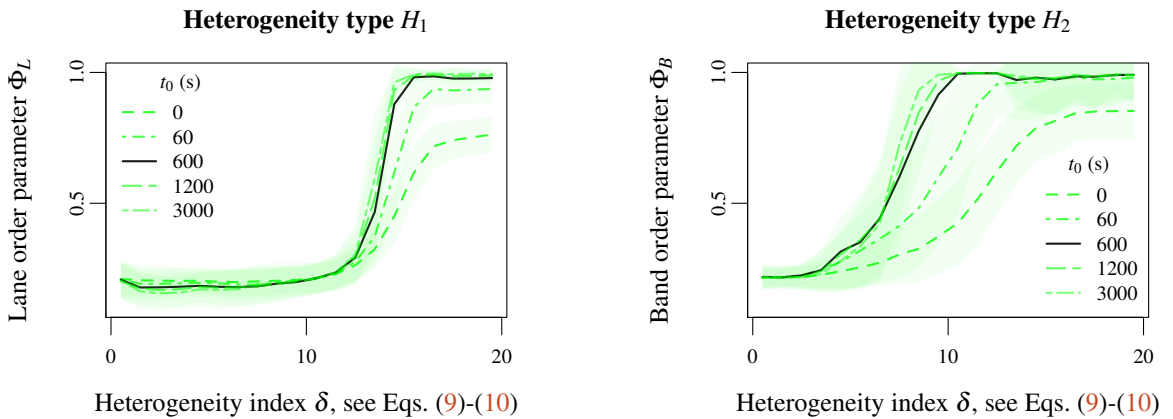


Figure 5 Lane order parameter for the model (5) (left panel) and band order parameter for the model (6) (right panel) for different waiting times t_0 before the measurements start. Lane and band formation emerge relatively fast (e.g. during the first minutes of simulation).

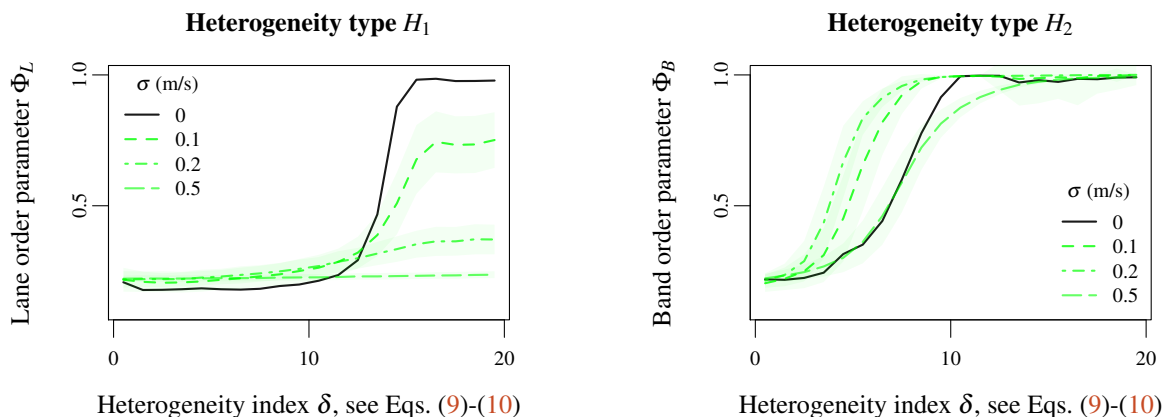


Figure 6 Lane order parameter for the model (5) (left panel) and band order parameter for the model (6) (right panel) for different noise amplitudes σ . The noise clearly affects the lane formation (left panel – freezing-by-heating-effect) while it can improve the band formation (right panel).

progressively breaking it as the noise increases (Fig. 6, right panel, $\sigma = 0.5$ m/s). The band pattern is not only robust to the noise, but in certain noise ranges band formation is improved.

In order to study the density dependence, simulations for different density regimes are performed, namely $\rho = 0.5$ (low density), $\rho = 1$ (middle) and $\rho = 2$ ped/m² (high density); see Fig. 7. A non-monotonous relationship between lane and band formation and the density level is observed. The density negatively impacts the lane formation while band formation especially arise for intermediate density levels. Note that the performances for high density level ($\rho = 2$ ped/m²) may not be stationary. Indeed, the time required to reach a stationary state increases as the number of agents increases.

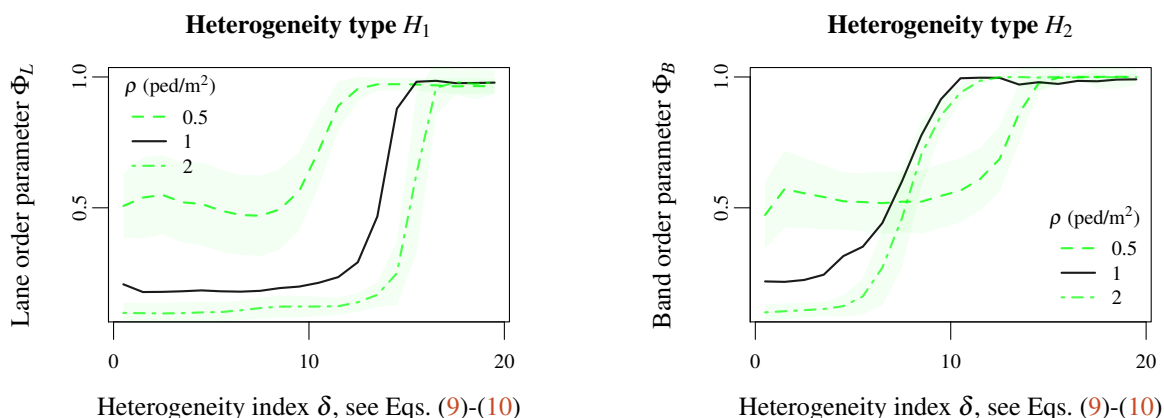


Figure 7 Lane order parameter for the model (5) (left panel) and band order parameter for the model (6) (right panel) for different density levels. Non-monotonous relationships exist between the lane and band formation and the density level.

4 Conclusion

We have compared the effects of two different microscopic heterogeneity mechanisms on the formation of collective segregation in two-species flows of polarised agents. In the case of the static heterogeneity type (5) where the heterogeneity is in the agent characteristics, the formation of longitudinal lanes is observed. For the dynamic type of heterogeneity (6) the heterogeneity is in the interactions. In this case, we find the generation of transversal bands. Both lanes and bands already emerge rather early in the simulations. The formation is not restricted to a specific density regime. The structures are partly robust to stochastic perturbations, especially the band formation. It can even be improved by perturbing the agent dynamics (freezing-by-heating effect). On the other hand, this is not possible for the lane formation. A similar behaviour is found in simulations where the noise is introduced in the agent polarity (i.e. the desired direction) instead of the speed. Such results corroborate the universality of lane formation observed in counter-flows [5] and opens new explanation perspectives for the formation of stripes and bands.

Acknowledgements RK and AT acknowledge the Franco-German research project MADRAS funded in France by the Agence Nationale de la Recherche (ANR, French National Research Agency), grant number ANR-20-CE92-0033, and in Germany by the Deutsche Forschungsgemeinschaft (DFG, German Research Foundation), grant number 446168800.

Additional information Simulations of lane and band formations can be implemented online on the dedicated webpage www.vzu.uni-wuppertal.de/fileadmin/site/vzu/Lane-and-band-formation. Programming code (in Logo language) can be downloaded on the same link.

References

- [1] Kirchner, A., Nishinari, K., Schadschneider, A.: Friction effects and clogging in a cellular automaton model for pedestrian dynamics. *Phys. Rev. E* **67**, 056122 (2003). [doi:10.1103/PhysRevE.67.056122](https://doi.org/10.1103/PhysRevE.67.056122)
- [2] Zuriguel, I., Parisi, D.R., Hidalgo, R.C., Lozano, C., Janda, A., Gago, P.A., Peralta, J.P., Ferrer, L.M., Pagnaloni, L.A., Clément, E.: Clogging transition of many-particle systems flowing through bottlenecks. *Sci. Rep.* **4**, 7324 (2014). [doi:10.1038/srep07324](https://doi.org/10.1038/srep07324)
- [3] Nicolas, A., Bouzat, S., Kuperman, M.N.: Pedestrian flows through a narrow doorway: Effect of individual behaviours on the global flow and microscopic dynamics. *Transp. Res. Part B Meth.* **99**, 30–43 (2017). [doi:10.1016/j.trb.2017.01.008](https://doi.org/10.1016/j.trb.2017.01.008)
- [4] Xu, Q., Chraïbi, M., Seyfried, A.: Prolonged clogs in bottleneck sim-

- ulations for pedestrian dynamics. *Physica A* **573**, 125934 (2021).
[doi:10.1016/j.physa.2021.125934](https://doi.org/10.1016/j.physa.2021.125934)
- [5] Cristin, J., Méndez, V., Campos, D.: General scaling in bidirectional flows of self-avoiding agents. *Sci. Rep.* **9**, 18488 (2019).
[doi:10.1038/s41598-019-54977-3](https://doi.org/10.1038/s41598-019-54977-3)
- [6] Goldsztein, G.H.: Self-organization when pedestrians move in opposite directions. multi-lane circular track model. *Appl. Sci.* **10**(2), 563 (2020).
[doi:10.3390/app10020563](https://doi.org/10.3390/app10020563)
- [7] Helbing, D., Farkas, I., Vicsek, T.: Freezing by heating in a driven mesoscopic system. *Phys. Rev. Lett.* **84**(6), 1240–1243 (2000).
[doi:10.1103/PhysRevLett.84.1240](https://doi.org/10.1103/PhysRevLett.84.1240)
- [8] Kirchner, A., Schadschneider, A.: Simulation of evacuation processes using a bionics-inspired cellular automaton model for pedestrian dynamics. *Physica A* **312**, 260–276 (2002). [doi:10.1016/S0378-4371\(02\)00857-9](https://doi.org/10.1016/S0378-4371(02)00857-9)
- [9] Bain, N., Bartolo, D.: Dynamic response and hydrodynamics of polarized crowds. *Science* **363**(6422), 46–49 (2019). [doi:10.1126/science.aat9891](https://doi.org/10.1126/science.aat9891)
- [10] Friesen, M., Gottschalk, H., Rüdiger, B., Tordeux, A.: Spontaneous wave formation in stochastic self-driven particle systems. *SIAM J. Appl. Math.* **81**(3), 853–870 (2021). [doi:10.1137/20M1315567](https://doi.org/10.1137/20M1315567)
- [11] Stanley, H.: Non-equilibrium physics: Freezing by heating. *Nature* **404**, 718 (2000).
[doi:10.1038/35008188](https://doi.org/10.1038/35008188)
- [12] Helbing, D., Buzna, L., Johansson, A., Werner, T.: Self-organized pedestrian crowd dynamics: Experiments, simulations, and design solutions. *Transp. Sci.* **39**(1), 1–24 (2005). [doi:10.1287/trsc.1040.0108](https://doi.org/10.1287/trsc.1040.0108)
- [13] Helbing, D., Johansson, A.: *Pedestrian, Crowd and Evacuation Dynamics*, pp. 6476–6495. Springer New York (2009).
[doi:10.1007/978-0-387-30440-3_382](https://doi.org/10.1007/978-0-387-30440-3_382)
- [14] Cividini, J., Appert-Rolland, C., Hilhorst, H.J.: Diagonal patterns and chevron effect in intersecting traffic flows. *EPL* **102**(2), 20002 (2013).
[doi:10.1209/0295-5075/102/20002](https://doi.org/10.1209/0295-5075/102/20002)
- [15] Chowdhury, D., Santen, L., Schadschneider, A.: Statistical physics of vehicular traffic and some related systems. *Phys. Rep.* **329**(4-6), 199–329 (2000).
[doi:10.1016/S0370-1573\(99\)00117-9](https://doi.org/10.1016/S0370-1573(99)00117-9)
- [16] Bellomo, N., Piccoli, B., Tosin, A.: Modeling crowd dynamics from a complex system viewpoint. *Math. Models Methods Appl. Sci.* **22**(supp02), 1230004 (2012).
[doi:10.1142/S0218202512300049](https://doi.org/10.1142/S0218202512300049)

- [17] Boltes, M., Zhang, J., Tordeux, A., Schadschneider, A., Seyfried, A.: Empirical Results of Pedestrian and Evacuation Dynamics, pp. 1–29. Springer, Berlin, Heidelberg (2018). [doi:10.1007/978-1-4939-8763-4_706](https://doi.org/10.1007/978-1-4939-8763-4_706)
- [18] Hermann, G., Touboul, J.: Heterogeneous connections induce oscillations in large-scale networks. *Phys. Rev. Lett.* **109**, 018702 (2012). [doi:10.1103/PhysRevLett.109.018702](https://doi.org/10.1103/PhysRevLett.109.018702)
- [19] Moussaïd, M., Kämmer, J.E., Analytis, P.P., Neth, H.: Social influence and the collective dynamics of opinion formation. *PLOS ONE* **8**(11), 1–8 (2013). [doi:10.1371/journal.pone.0078433](https://doi.org/10.1371/journal.pone.0078433)
- [20] Touboul, J.D.: The hipster effect: When anti-conformists all look the same. *Discrete Continuous Dyn. Syst. Ser. B* **24**, 4379 (2019). [doi:10.3934/dcdsb.2019124](https://doi.org/10.3934/dcdsb.2019124)
- [21] Shahhoseini, Z., Sarvi, M.: Collective movements of pedestrians: How we can learn from simple experiments with non-human (ant) crowds. *PLOS ONE* **12**, 1–20 (2017). [doi:10.1371/journal.pone.0182913](https://doi.org/10.1371/journal.pone.0182913)
- [22] Needleman, D., Dogic, Z.: Active matter at the interface between materials science and cell biology. *Nat. Rev. Mater.* **2**(9), 1–14 (2017). [doi:10.1038/natrevmats.2017.48](https://doi.org/10.1038/natrevmats.2017.48)
- [23] Cerotti, D., Distefano, S., Merlino, G., Puliafito, A.: A crowd-cooperative approach for intelligent transportation systems. *IEEE Trans. Intell. Transp. Syst.* **18**(6), 1529–1539 (2017). [doi:10.1109/TITS.2016.2609606](https://doi.org/10.1109/TITS.2016.2609606)
- [24] Nakayama, A., Hasebe, K., Sugiyama, Y.: Instability of pedestrian flow and phase structure in a two-dimensional optimal velocity model. *Phys. Rev. E* **71**, 036121 (2005). [doi:10.1103/PhysRevE.71.036121](https://doi.org/10.1103/PhysRevE.71.036121)
- [25] Moussaïd, M., Guillot, E., Moreau, M., Fehrenbach, J., Chabiron, O., Lemerrier, S., Pettré, J., Appert-Rolland, C., Degond, P., Theraulaz, G.: Traffic instabilities in self-organized pedestrian crowds. *PLOS Comput. Biol.* **8**(3), 1–10 (2012). [doi:10.1371/journal.pcbi.1002442](https://doi.org/10.1371/journal.pcbi.1002442)
- [26] Feliciani, C., Murakami, H., Nishinari, K.: A universal function for capacity of bidirectional pedestrian streams: Filling the gaps in the literature. *PLOS ONE* **13**, 1–31 (2018). [doi:10.1371/journal.pone.0208496](https://doi.org/10.1371/journal.pone.0208496)
- [27] Fujita, A., Feliciani, C., Yanagisawa, D., Nishinari, K.: Traffic flow in a crowd of pedestrians walking at different speeds. *Phys. Rev. E* **99**, 062307 (2019). [doi:10.1103/PhysRevE.99.062307](https://doi.org/10.1103/PhysRevE.99.062307)
- [28] Sun, Y.: Kinetic Monte Carlo simulations of bi-direction pedestrian flow with different walk speeds. *Physica A* **549**, 124295 (2020). [doi:10.1016/j.physa.2020.124295](https://doi.org/10.1016/j.physa.2020.124295)

- [29] Schwarting, W., Pierson, A., Alonso-Mora, J., Karaman, S., Rus, D.: Social behavior for autonomous vehicles. *Proc. Natl. Acad. Sci. U.S.A.* **116**(50), 24972–24978 (2019). doi:10.1073/pnas.1820676116
- [30] Stern, R.E., Cui, S., Monache, M.L.D., Bhadani, R., Bunting, M., Churchill, M., Hamilton, N., Haulcy, R., Pohlmann, H., Wu, F., Piccoli, B., Seibold, B., Sprinkle, J., Work, D.B.: Dissipation of stop-and-go waves via control of autonomous vehicles: Field experiments. *Transp. Res. Part C Emerg. Technol.* **89**, 205–221 (2018). doi:10.1016/j.trc.2018.02.005
- [31] Tordeux, A., Chraïbi, M., Seyfried, A.: Collision-free speed model for pedestrian dynamics. In: *Traffic and Granular Flow '15*, pp. 225–232. Springer, Cham (2016). doi:10.1007/978-3-319-33482-0_29
- [32] Krüsemann, H., Godec, A., Metzler, R.: First-passage statistics for aging diffusion in systems with annealed and quenched disorder. *Phys. Rev. E* **89**(4), 040101 (2014). doi:10.1103/PhysRevE.89.040101
- [33] Tateishi, A., Ribeiro, H., Sandev, T., Petreska, I., Lenzi, E.: Quenched and annealed disorder mechanisms in comb models with fractional operators. *Phys. Rev. E* **101**(2), 022135 (2020). doi:10.1103/PhysRevE.101.022135
- [34] Rex, M., Löwen, H.: Lane formation in oppositely charged colloids driven by an electric field: Chaining and two-dimensional crystallization. *Phys. Rev. E* **75**, 051402 (2007). doi:10.1103/PhysRevE.75.051402
- [35] Coville, F.V.: The influence of cold in stimulating the growth of plants. *J. Agric. Res* **20**(2), 151–160 (1920). doi:10.1073/pnas.6.7.434
- [36] L. Radzihovsky, N.C.: Comment on "freezing by heating in a driven mesoscopic system. *Phys. Rev. Lett.* **90**, 189603 (2003). doi:10.1103/physrevlett.90.189603
- [37] Borchers, N., Pleimling, M., Zia, R.K.: Non-equilibrium statistical mechanics of a two-temperature ising ring with conserved dynamics. *Phys. Rev. E* **90**, 062113 (2014). doi:10.1103/PhysRevE.90.062113
- [38] Jejjala, V., Kavic, M., Minic, D., Tze, C.H.: The Big Bang as the ultimate traffic jam. *Int. J. Mod. Phys. D* **18**, 2257 (2009). doi:10.1142/S021827180901593X
- [39] Zia, R., Praestgaard, E., Mouritsen, O.: Getting more from pushing less: Negative specific heat and conductivity in non-equilibrium steady states. *Am. J. Phys.* **70**, 384 (2002). doi:10.1119/1.1427088
- [40] Sørdal, V., Bergli, J., Galperin, Y.: Cooling by heating: restoration of the third law of thermodynamics. *Phys. Rev. E* **93**, 032102 (2016). doi:10.1103/PhysRevE.93.032102